Lecture 3: Superresolution imaging using Subwavelength Resonances

Hai Zhang
HKUST

11-th Zurich Summer School, Aug 23-27, 2021

Sensitivity of sensing using hole structures

Joint work with Junshan Lin from Auburn University:

Sensitivity of resonance frequency in the detection of thin layer using nano-slit structures, IMA Journal of Applied Mathematics , 2021.

Motivation: Biosensing

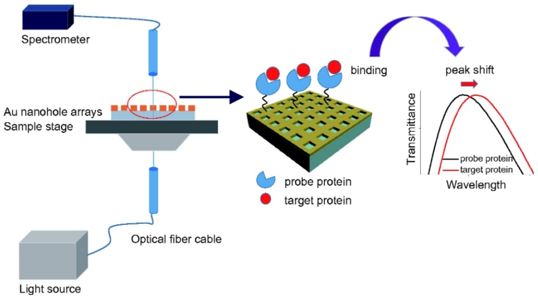

References: A. Cetin, *et al* (2015), A. Blanchard-Dionne and M. Meunier (2017), J. Gomez-Cruz, *et al* (2018), S. Oh and H. Altug (2018), $\cdots$

Mathematical questions:

- Characterize the spectral sensitivity in the detection of thin biochemical layer.
- Identify the main features of the samples from resonance frequencies and their shifts (Inverse Spectral Problems).

Spectral sensitivity analysis

$$\frac{dk(H)}{dH} = O(1+|\log(H/\delta)|) \quad \text{if } H \lesssim \delta \quad \text{and} \quad \frac{dk(H)}{dH} = O\left(\frac{\delta}{H}\right) \quad \text{if } H \gtrsim \delta$$

where $k(H)$ is the resonant frequency.

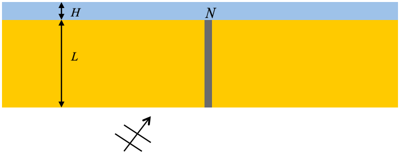

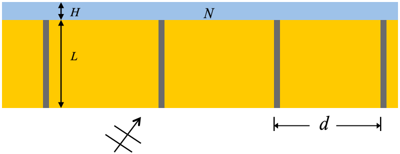

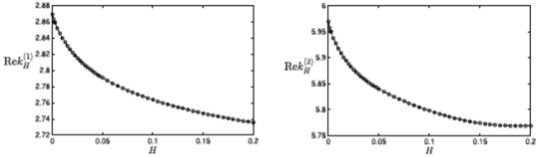

FIG. 5. The resonance frequencies $\mathrm{Re}k_H^{(1)}$ and $\mathrm{Re}k_H^{(2)}$ for various thickness $H \in [10^{-5}, 0.2]$ when $\delta = 0.05$. The period $d = 1.2$, the Bloch wave number $\kappa = 0$ and the permittivity values $\varepsilon_\ell = 2$, $\varepsilon_s = 1$.

Superresolution imaging of thin objects using hole structures

Joint work with Junshan Lin from Auburn University:

Super-resolution imaging via subwavelength hole resonances,

Physical Review Applied, 2020.

The roadmap for super-resolution imaging I

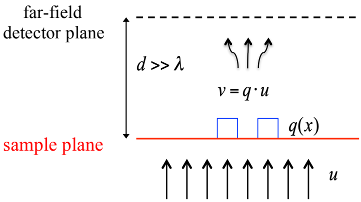

Imaging in an ideal scenario in 2D:

- The thin sample is characterized by the transmission function $q(x)$
- The incident field u satisfying $\Delta u + k^2 u = 0$ generates an illumination pattern on the sample plane.
- v is the transmitted field at the sample plane.
- Goal: Recover q from the far-field data.
- Diffraction limit: far-field data is given by $\hat{v}(\xi)$ for $\xi \in (-k, k)$. If u is a plane wave, then the illumination pattern only has Fourier component for $|\xi| < k$. One can only retrieve the Fourier component of q for $|\xi| < 2k$.
- Idea of superresolution: generate high-oscillatory illumination pattern on the sample plane.

- Example $u_m = e^{imkx - \zeta y}$ with $(mk)^2 - \zeta^2 = k^2$, $m = \pm 2, \pm 3, \cdots, \pm M$ then

$$\hat{v}_m(\xi, 0) = \hat{u}_m(\xi, 0) * \hat{q}(\xi) = \hat{q}(\xi - mk) \quad \text{for } \xi \in (-k, k).$$

- $\hat{q}(\xi)$ for $\xi \in [-(M+1)k, (M+1)k]$ can be recovered

The roadmap for super-resolution imaging II

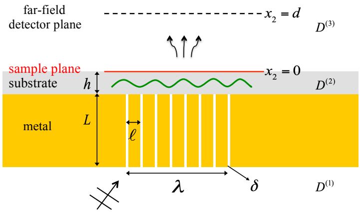

- An array of identical slit holes $S_1, S_2, \cdots, S_J$ are patterned in a metallic slab, with $\delta \ll \ell < \lambda/2$.
- Apply the resonant modes generated from subwavelength hole as the illumination patterns.
- By tuning the incidence at resonant frequencies, the subwavelength holes generate strong wave field with desired oscillation patterns.
- The substrate is needed to control the shift of resonant frequencies caused by the sample.

Resonance for subwavelength holes I

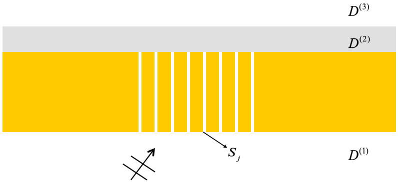

- The total field u satisfies

$$
\begin{cases}
\nabla \cdot \left(\dfrac{1}{\varepsilon(x)} \nabla u \right) + k^2 u = 0 \qquad \text{in } D, \\
\text{where } D := D^{(1)} \cup D^{(2)} \cup D^{(3)} \cup (\cup_{j=1}^{J} S_j); \\
\dfrac{\partial u}{\partial \nu} = 0 \quad \text{on } \partial D^{(1)}.
\end{cases}
$$

- $u_{\mathrm{diff}} := u - u_{\mathrm{inc}}$ satisfies the outgoing radiation conditions at infinity.

- The complex-valued resonances can be obtained by using layer potential techniques.

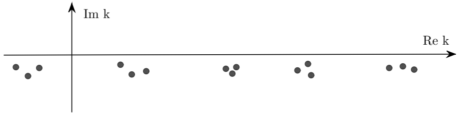

- The transmitted field adopts the expansion

$$u(x) = \sum_{j=1}^{J} a_j \cdot g(x, x_j) + O(\delta^\beta),$$

where x_j is located at the j'th slit aperture.

Transmitted field above the sample plane at the resonant frequencies $k = \Re\, k_{1j}$ for $j = 1, 2, \cdots$

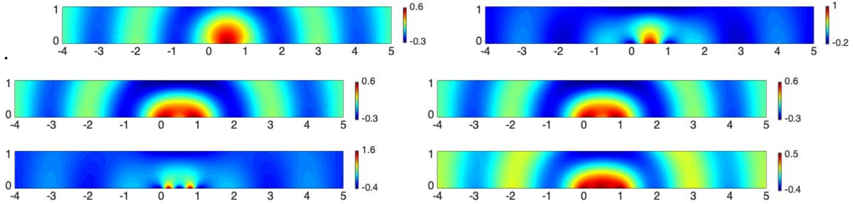

Wave patterns at resonant frequencies

Transmitted field on the sample plane at the resonant frequencies $k = \Re\, k_{1j}$ for $j = 1,\, 2,\, \cdots,\, 6$

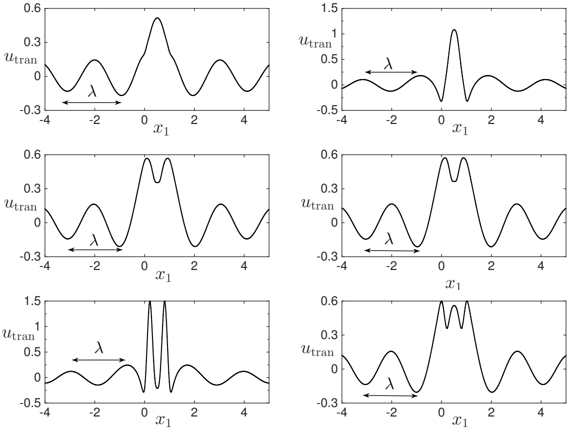

Strong transmitted field with desired oscillation patterns

Super-resolution imaging of infinitely thin samples I

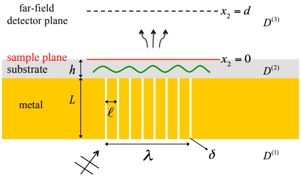

- $u_{\rm tran}$: transmitted field on the sample plane through the subwavelength holes
- $q(x_1)$: transmission function of an infinitely thin layer
- $u_{\rm samp}(x_1,0) = q(x_1)u_{\rm tran}(x_1,0)$: wave field transmitted immediately through the sample
- The propagation of the sample field $u_{\rm samp}$ to the detection plane is described by the propagator (transfer function) in the Fourier domain:

$$\hat{u}_{\rm det}(\xi, d) = e^{i\rho_0(\xi)d}\,\hat{u}_{\rm samp}(\xi, 0),$$

where

$$\rho_0(\xi) = \begin{cases} \sqrt{k^2\varepsilon_0 - \xi^2}, & |\xi| \le k, \\ i\sqrt{\xi^2 - k^2\varepsilon_0}, & |\xi| > k. \end{cases}$$

- The relation in the spatial domain:

$$u_{\rm det}(\cdot, d) = w_d * u_{\rm samp} = w_d * (q \cdot u_{\rm tran}), \quad \text{where } \hat{w}_d(\xi) = e^{i\rho_0(\xi)d}.$$

Super-resolution imaging of infinitely thin samples II

- Define the forward operator $A_k[p] := w_d * (p \cdot u_{\mathrm{tran}})$.
- h_k and $h_k^{(0)}$: measurement when the sample is present and not, respectively.
- Recover $p := 1 - q$ by solving the equation

$$A_k[p] + \eta_k = g_k, \quad \text{where } g_k := h_k - h_k^{(0)}, \eta_k \text{ is the noise.}$$

- For multiple frequency configuration, solve the equation $A[p] + \eta = g$, where

$$A = \begin{bmatrix} A_{k_1} \\ \cdot \\ \cdot \\ \cdot \\ A_{k_m} \end{bmatrix}, \quad g = \begin{bmatrix} g_{k_1} \\ \cdot \\ \cdot \\ \cdot \\ g_{k_m} \end{bmatrix}, \quad \text{and} \quad \eta = \begin{bmatrix} \eta_{k_1} \\ \cdot \\ \cdot \\ \cdot \\ \eta_{k_m} \end{bmatrix}.$$

- Two numerical approaches: Gradient descent method and Total variation regularization.

Numerical examples

A total of 9 slit holes span about 2λ such that the neighboring slit distance $\ell \approx \lambda/4$; The measurement distance is 5λ, 5% Gaussian random noise.

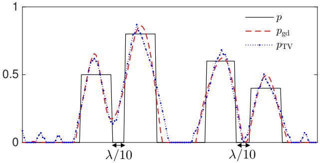

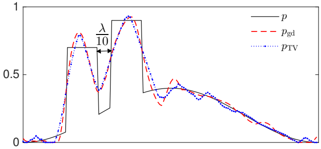

A total of 9 slit holes span about λ and $\ell \approx \lambda/8$.

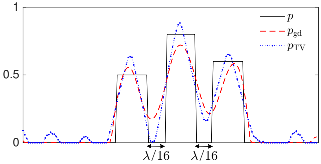

Image resolution $\approx \ell/2$.

Super-resolution imaging of thin samples with finite thickness

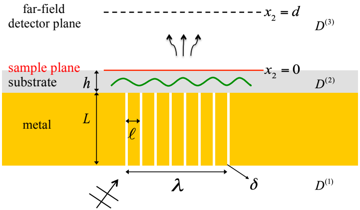

- Born approximation:

$$\Delta u_{\mathrm{diff}} + k^2 u_{\mathrm{diff}} = -k^2 \left(\varepsilon(x) - 1\right) u_{\mathrm{tran}} \quad \text{in } D^{(3)},$$

.

- The forward operator:

$$A_k[p] = -k^2 \int_{R_0} g^{(3)}(x_1, d; y) u_{\mathrm{tran}}(y)\, p(y) dy, \quad p = \varepsilon - 1.$$

- Gradient descent and total variation regularizations are applied.

Numerical examples

The neighboring slit distance $\ell \approx \lambda/4$.

Top: real image; middle: gradient reconstruction; bottom: TV regularization

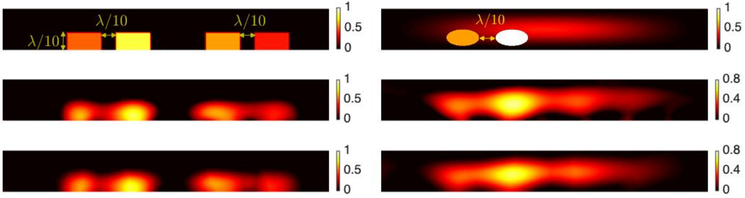

The neighboring slit distance $\ell \approx \lambda/8$

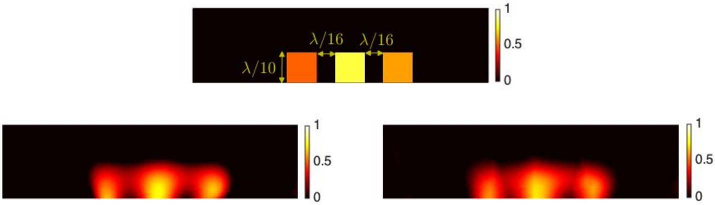

Summary and outlook

Summary: Subwavelength holes can be used to generate illumination patterns which can probe both the high and low spacial frequency components of imaging targets to achieve superresolution.

Outlook

1. Real metallic structures and 3D subwavelength structures: quantitative analysis and numerical approach

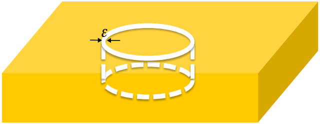

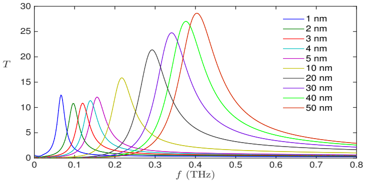

2. Applications in biosensing and imaging (inverse problems).

Reconstruct small objects beyond the resolution limit: plasmonic sensing

Joint work with H. Ammari, M. Ruiz, S. Yu:
SIAM Journal on Imaging Sciences, 2018

Plasmonic sensing

1. Reconstruct (or classify) a small object from far field measurements.
2. The inverse problem is severally ill-posed because of the diffract limit and low signal-to-noise ratio (SNR).
3. Idea: Plasmonic sensing.

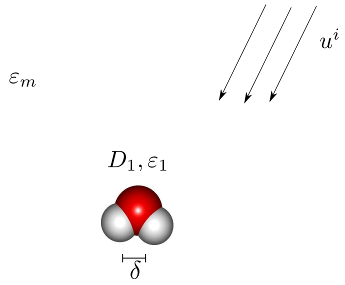

Plasmonic nanoparticles

1. Metallic particle (typically made of gold) whose size range from several nm's to a hundred of nm's;
2. The free electron density of the plasmonic particle can be strongly coupled to EM fields at surface plasmon resonant frequencies in the visible and near-infrared regime, and results strong resonant scattering.

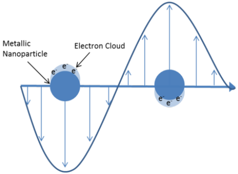

$$\begin{cases} \nabla \cdot \frac{1}{\epsilon_D} \nabla u = 0 \quad \text{in } \mathbb{R}^3, \\ \epsilon_D = \epsilon_m \chi(\mathbb{R}^3 \setminus \bar{D}) + \epsilon_c \chi(\bar{D}), \\ \epsilon_c = 1 - \frac{\omega_p^2}{\omega(\omega + i\gamma_p)}. \end{cases}$$

Plasmon resonance: Quasi-static model (the far field)

Define the contrast parameter:

$$\lambda = \lambda(\omega) = \frac{\epsilon_m + \epsilon_c(\omega)}{2(\epsilon_m - \epsilon_c(\omega))}.$$

Theorem

The solution u has the following asymptotic

$$u(x) = u^i(x) + \nabla_y G(x, 0) \cdot M(\lambda, D) \nabla u^i(0) + O\left(\frac{\delta^{d+1}}{\mathrm{dist}(\lambda, \sigma(\mathcal{K}_D^*))}\right),$$

where $\sigma(\mathcal{K}_D^*) = \{\lambda_1, \lambda_2, \cdots .\}$ denotes the spectrum of $\mathcal{K}_D^*$ (The Nuemann-Poicare operator associated with the domain D) in $\mathcal{H}^*(\partial D)$ and

$$M(\lambda, D) = \sum_{j=1}^{\infty} \frac{(\nu_l, \varphi_j)_{\mathcal{H}^*} (\varphi_j, x_m)}{\lambda - \lambda_j}$$

is the polarization tensor associated with D.

For a domain D with $C^{1,\alpha}$ boundary, we define

$$\mathcal{K}_D^*\psi(x) = \frac{1}{\omega_d} p.v. \int_{\partial D} \frac{< y - x, \nu(y) >}{|x-y|^d} \psi(y) d\sigma(y)$$

where d is the dimension of the space and ω_d is the area of the unit sphere in $\mathbf{R}^d$.

Lemma

1. *$\mathcal{K}_D^*$ is compact from $L^2(\partial D)$ to $L^2(\partial D)$ and is self-adjoint in $H^{-\frac{1}{2}}(\partial D)$ equipped with the following inner product*

$$(u, v)_{\mathcal{H}^*} = -(u, \mathcal{S}_D[v])_{-\frac{1}{2},\frac{1}{2}}.$$

2. *The following presentation formula holds: for any $\psi \in H^{-1/2}(\partial D)$, $\mathcal{K}_D^* = \sum_{j=0}^{\infty} \lambda_j (\cdot, \varphi_j)_{\mathcal{H}^*} \otimes \varphi_j, \quad$ where $-\frac{1}{2} < \lambda_j \leq \frac{1}{2}$.*

We denote the space $H^{-\frac{1}{2}}(\partial D)$ with the new inner product by $\mathcal{H}^*(\partial D)$.

Plasmonic resonances

Plasmonic resonances depend on[1]:

1. The shape, size and the physical properties of the particle;
2. The physical properties of the background media.

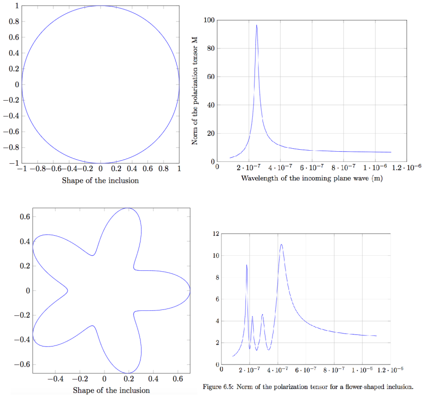

Figure 6.5: Norm of the polarization tensor for a flower-shaped inclusion.

[1] Mathematical analysis of plasmonic nanoparticles: the scalar case, Ammari, Millien, Ruiz and Z, ARMA, 2017.

Plasmonic sensing

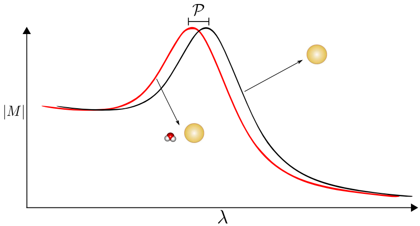

Main Idea: By using the near field interaction with a known plasmonic particle (sensor), the fine detail information of the small object can be encoded into the shift of the resonant frequencies.

Two interaction regimes

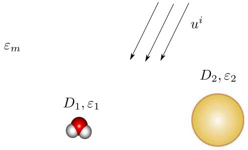

Intermediate interaction regime:

i) The plasmonic particle D_2 has size of order one; the ordinary particle $D_1 = \delta B$ has size of order $\delta \ll 1$.

ii) $\mathrm{dist}(D_1, D_2)$ is of order one.

Strong interaction regime:

i) The plasmonic particle D_2 has size of order one; the ordinary particle $D_1 = \delta B$ has size of order $\delta \ll 1$.

ii) there exist positive constants C_1 and C_2 such that $C_1 < C_2$ and

$$C_1\delta \le \mathrm{dist}(D_1, D_2) \le C_2\delta.$$

Shift in the plasmonic resonance in the intermediate regime

Thm: The following expansion holds in the far field:

$$u(x) = u^i(x) + \nabla u^i(z) \cdot M(\lambda_{D_2}, D_1, D_2) \nabla G(x,z) + O\left(\frac{\delta^{d+1}}{\mathrm{dist}(\lambda, \sigma(\mathcal{K}^*_{D_2}))} \right),$$

where

$$M(\lambda_{D_2}, D_1, D_2)_{l,m} = \sum_{j=1}^{\infty} \frac{(\nu_l, \varphi_j)_{\mathcal{H}^*} (\varphi_j, x_m)_{-\frac{1}{2},\frac{1}{2}}}{\lambda_{D_2} - \lambda_j + \mathcal{P}_j},$$

$$\lambda_{D_2} = \frac{\epsilon_2 + \epsilon_m}{2(\epsilon_2 - \epsilon_m)}.$$

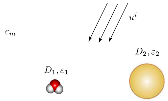

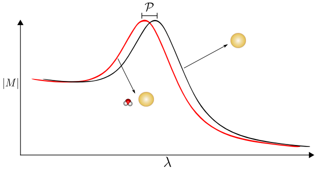

Shift in the plasmonic resonance in the intermediate regime

Thm: In the intermediate interaction regime,

$$\begin{aligned}\mathcal{P}_j &= R_{jj} + \sum_{l\neq j} \frac{R_{jl}R_{lj}}{\lambda_j-\lambda_l} + \sum_{(l_1,l_2)\neq j} \frac{R_{jl_2}R_{l_2l_1}R_{l_1j}}{(\lambda_j-\lambda_{l_1})(\lambda_j-\lambda_{l_2})} + \ldots,\\ R_{jl} &= \left(\frac{1}{2}-\lambda_j\right)\sum_{m=1}^{M}\sum_{n=1}^{N} a_m^j M_{m,n}(D_1)(a_n^l)^t + O(\delta^{M+N+1}),\end{aligned}$$

where $M_{m,n}(D_1)$'s are the generalized polarization tensors of the object D_1.

Thm (Ammari-Lim-Kang-Zaribi): For D of type $C^{1,\alpha}$ and $\lambda \in \mathbb{C}$, the set $M_{m,n}(\lambda, D)$ define uniquely λ and D.

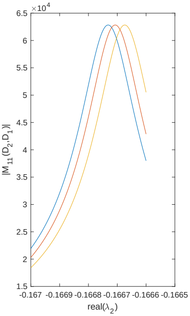

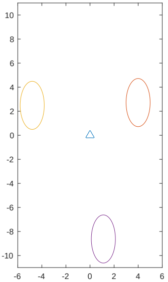

Inverse problem of plasmonic sensing

Assume that the plasmonic resonance occurs at λ_1.
We consider two steps:

1) Recover the first order CGPTs from measurements of $\mathcal{P}_1$ for different positions of the plasmonic nanoparticle.
2) An optimal control approach to estimate the shape of D_1.

Numerical results in the intermediate regime

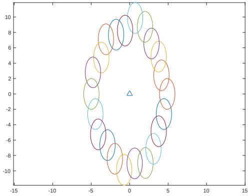

Positions of D_2 for which we measure $\mathcal{P}_1$.

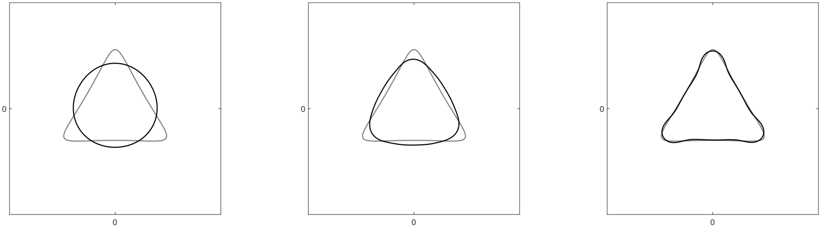

Plasmonic sensing in the strong interaction regime

Remark: The perturbation argument fails in the strong interaction case, shift in resonant frequency in not small.

Main approach: design a conformal mapping which transforms the two particle system into a shell-core structure. Perturbation argument can be used to analyze the shift in the resonant frequencies due to the presence of the inner dielectric core.

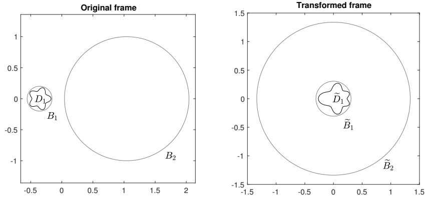

Example: shifts in plasmonic resonance

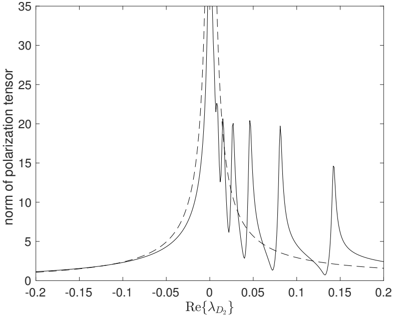

The dotted line: without dielectric particle;
The solid line: with a dieletric particle D_1.

The strong interaction regime

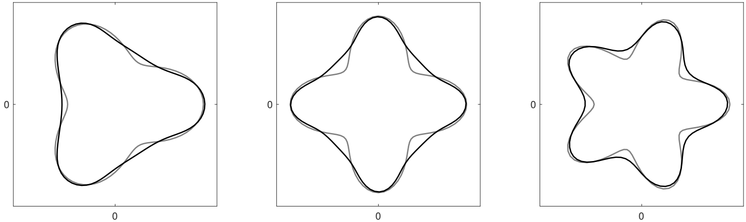

Gray curves: the original shape;
Black curves: the reconstructed shape. The iteration number is 30.

References:

1. Reconstructing fine details of small objects by using plasmonic spectroscopic data, Ammari, Ruiz, Yu and Z, SIAM Journal on Imaging Sciences, 2018.
2. Reconstructing fine details of small objects by using plasmonic spectroscopic data, Ammari, Ruiz, Yu and Z, SIAM Journal on Imaging Sciences, 1-23, 11, 2018.

Thank You!